

Flow Visualization of Angled Supersonic Jets into a Supersonic Cross Flow

Yan Shao, Jin Zhou, Lin Lai, Haiyan Wu and Jing Lei

Abstract—This paper describes Nano-particle based Planar Laser Scattering (NPLS) flow visualization of angled supersonic jets into a supersonic cross flow based on the HYpersonic Low TEMperature (HYLTE) nozzle which was widely used in DF chemical laser. In order to investigate the non-reacting flowfield in the HYLTE nozzle, a testing section with windows was designed and manufactured. The impact of secondary fluids orifice separation on mixing was examined. For narrow separation of orifices, the secondary fuel penetration increased obviously compared to diluent injection, which means smaller separation of diluent and fuel orifices would enhance the mixing of fuel and oxidant. Secondary injections with angles of 30, 40 and 50 degrees were studied. It was found that the injectant penetration increased as the injection angle increased, while the interfacial surface area to entrain the freestream fluid is largest when the injection angle is 40 degree.

Keywords—HYLTE nozzle, NPLS, supersonic mixing, transverse injection

I. INTRODUCTION

CURRENT combustion driven continuous wave DF chemical laser, to a large extent, employ HYpersonic Low TEMperature (HYLTE) nozzle in which fuel deuterium (D_2) and diluent helium (He) are injected obliquely into a primary stream containing rich oxidizer fluorine atoms through secondary nozzles at the expansion section of this nozzle. Then a high concentration of excited DF molecules is produced in the cavity by rapid, efficient mixing and combustion of fuel and oxidizer [1]. It has been found that the mixing phenomenon in HYLTE nozzle has a significant effect on the performance of DF chemical laser [2]. In order to optimize the nozzle design and the lasing efficiency, it is necessary to get a clear understanding of how the gaseous injections interact with the primary flow.

Nano-particle based Planar Laser Scattering (NPLS) has been newly developed based on Particle Image Velocimetry (PIV) technology by Shihe Yi and Yuxin Zhao of National University of Defense Technology [3]. As an advanced non-intrusive method for supersonic flow visualization, NPLS has the ability to investigate the fluid mechanics of HYLTE nozzle with supersonic angled injections. It is known that streamwise vortices produced by the interaction of injections and mainstream dominate and accelerate mixing. NPLS technique provides convenient conditions of the observation of streamwise vortices development of supersonic mixing.

Yan Shao, Jin Zhou, Lin Lai, Haiyan Wu and Jing Lei is with College of Aerospace and Material Engineering, National University of Defense Technology, Changsha, Hunan, China (corresponding author Yan Shao, e-mail: freebird_18@163.com).

II. EXPERIMENTAL SETUP

A. NPLS Technology

NPLS uses nanometer TiO_2 and pulsed planar laser as tracer particles and illumination respectively, not only solving the problem of particles flow-following but also improving the Signal-to-Noise of supersonic flow imaging. Due to the good flow-following ability of nanoparticles, if the concentration distribution of particles on the inlet of flowfield is uniform, the variation of particle will reflect the density variation and mixing structure of the flowfield. Thus the NPLS method is appropriate for the study of transverse injection of the HYLTE nozzle in which the density and concentration gradient are rather large.

The NPLS system consists of a computer, synchronizer, CCD camera, pulse laser and nanoparticle generator, the structure of which is schematically shown in Fig. 1. In NPLS, the computer controls the collaboration of the components and receives the experimental images. The input and output parameters of the synchronizer are controlled by software, collaboration of other components is controlled by signal of the synchronizer. The timing diagrams of exposure of CCD and laser output of pulse laser can be adjusted according to the purpose of measurement. The laser beam is transformed to a sheet with cylindrical lens. The nanoparticle generator is driven by high pressure gas, and the output particles concentration can be adjusted precisely by the driving pressure. While measuring the flowfield with NPLS, the nanoparticles are injected into and mixed with the inflow of the flowfield, while the flow is established in observing widow, the synchronizer controls the laser pulse and CCD to ensure synchronization of the emission of scattering laser by nanoparticles and the exposure of CCD.

The synchronizer has eight output ports with temporal precision at 0.25ns. The CCD is an interline transfer CCD equipped with micro-lens, of which the frame straddle time is adjustable (the shortest is 200ns) and is set as 5 μ s in this study.

The number of CCD array is 2000 \times 2000 pixels with 4096 grayscale grades. The pulse laser is a double pulse Nd:YAG laser, the wavelength of the laser is 532nm with duration of 6ns and 350mJ per pulse. The location of light sheet lens, polarization angle of laser, and particle flow rate of nanoparticle generator can be adjusted according to experimental requirements.

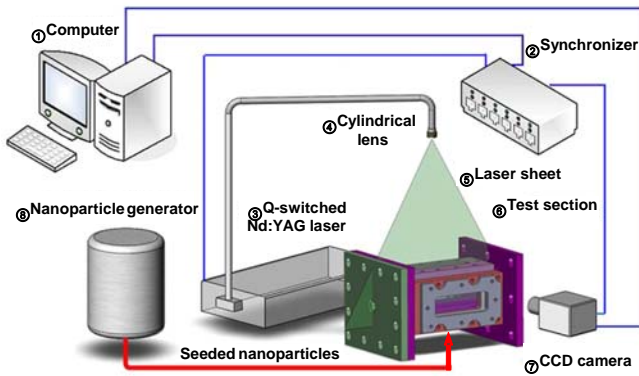


Fig. 1 Schematic diagram of NPLS system

B. HYLTE Nozzle Testing Section

In order to visualize the non-reacting flowfield of supersonic angled jets into a supersonic cross flow in the HYLTE nozzle, a testing section with observation windows is designed and manufactured, which is shown in Fig. 2. Three pieces of quartz

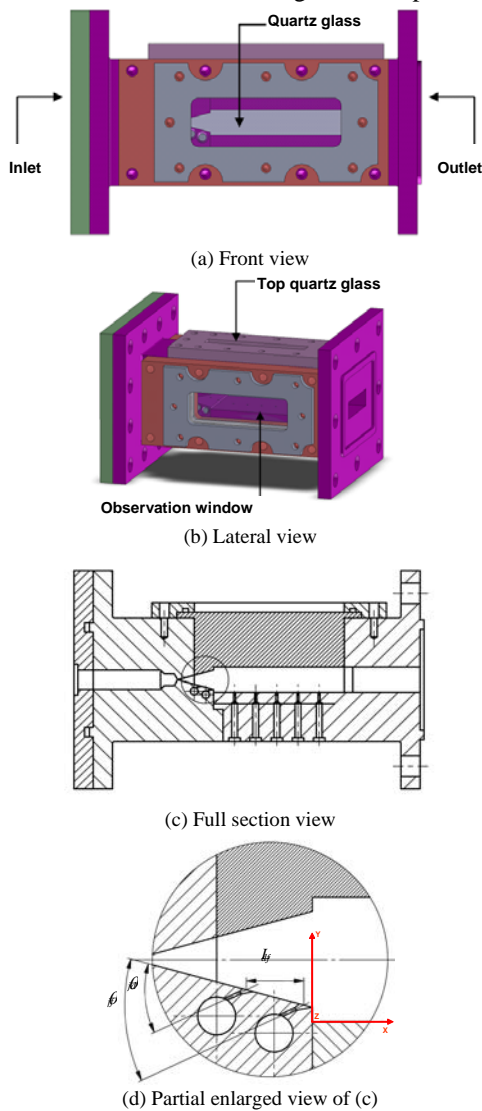


Fig. 2 HYLTE nozzle testing model

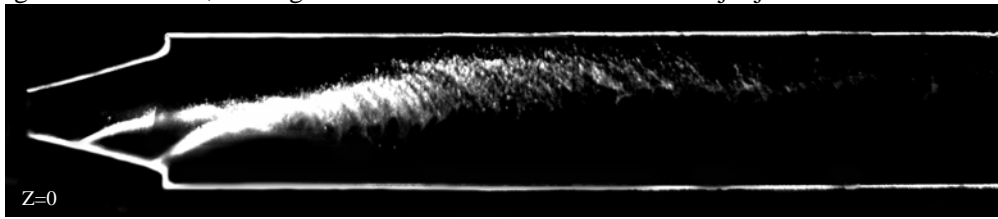
glass are embedded in the top and side observation windows respectively for the convenience of capturing the NPLS images of side view of midline plane, top view at wall-parallel plane and planes in several spanwise locations. As for HYLTE nozzle, mixing enhancement is mostly characterized for the variation of several flow control and geometrical parameters. We just pay attention to the latter one in this paper. It is pointed that secondary fluids injection angle θ_i and orifice separation L_{dj} are the key parameters which will determine the direction of the secondary gases injected into the primary stream, and the initial position of the reaction of fuel and oxidant taking place [4]. They could be changed by replacing the forefront of the nozzle component. Gas feeding and pressure measuring orifices are placed at the bottom of the testing section. The diffuser is installed at the end of the testing section which connects with vacuum tank and provides equivalent pressure between them. As for cold experiment, gaseous nitrogen is used to simulate the jet fluids of secondary nozzle and the cross flow of primary nozzle. Because secondary jets are 0.3mm in diameter, the tiny gaseous flow mixed with nanoparticles is dominated by mass flow controller (MFC).

III. RESULTS AND DISCUSSIONS

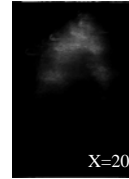
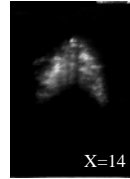
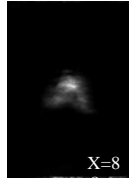
The function of the primary nozzle is to establish a supersonic flow, to create a low pressure low temperature environment which is appropriate for lasing. Its expansion ratio is 40. The total pressure of main stream is 0.42MPa and total temperature is 300K on average. As for secondary jets, the total pressure is 0.44MPa and total temperature is about 300K. The exit Mach number for the secondary diluent nozzle is 3.85, and for the secondary fuel nozzle is 3.58. The results that follow are separated into those from side-view, end-view (for nozzle A-E) and top-view (for nozzle A) imaging arrangements. It should be noted that each image is obtained from an individual experiment. Side-view images offer a view of the jet/crossflow and jet/jet interactions at the centerline of the twin injectors. Owing to the block effect of the first injector to the main flow, the second injector has a stronger injection and deeper penetration than the former injector. For the Mach number of the mainstream is a little too high (Mach 4-5), shear-induced mixing is poor [5], the mixing layer tends to become stable, as a result, some large-scale structures of the flowfield have been restrained. Results also show that the mixing quality is greatly enhanced by jet surface stretching and entraining the cross flow fluid continuously, which is clearly visualized in Fig. 3a. Considering that the second injector is immovable, the orifice separation can be changed by placing the first injector along the divergent section of HYLTE nozzle. For the narrow jet gap case (Fig. 4a), the front jet which is placed upstream of the second jet in supersonic cross flow acts to shield the latter one from the force of the oncoming fluid. For the downstream jet is located in the low pressure region behind the front jet, it penetrates higher through the primary stream than the former one. When the orifice

separation is increased (Fig. 5a), the penetration of the secondary fuel jet is increased for the shield effect is stronger, since the low pressure region between the two jets becomes larger. Furthermore, this region is situated at

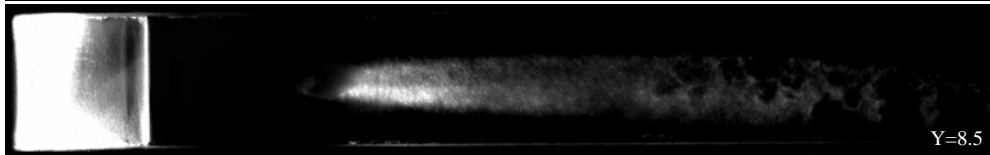
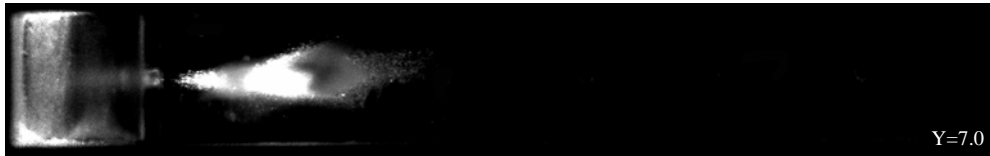
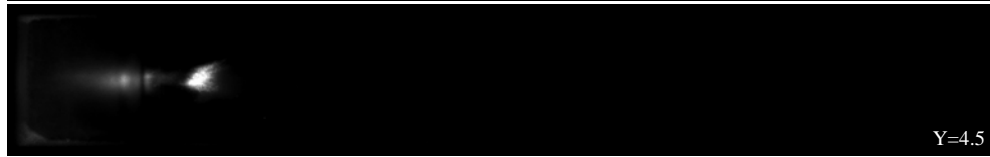
the diverging section of the primary nozzle, the low pressure condition could be sustained. But it is not suggested that the mixing is better for the wider jet gap case because the jet/jet is weaker.



a) Instantaneous side-view NPLS images

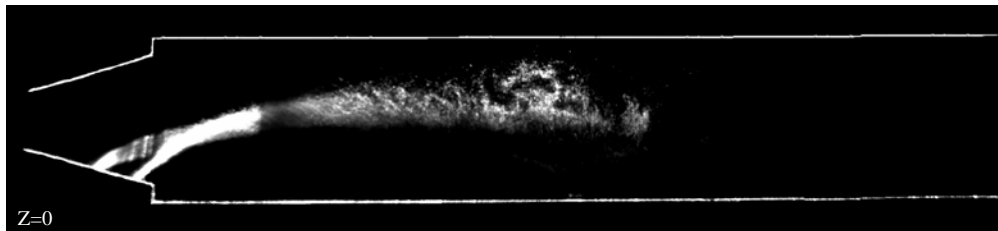


b) Instantaneous end-view NPLS images

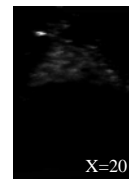
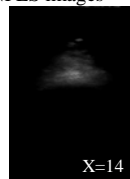
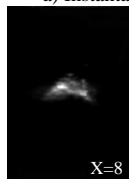


c) Instantaneous top-view NPLS images

Fig. 3 Nozzle A ($\theta_j = 40^\circ$, $L_{df} = 6mm$)

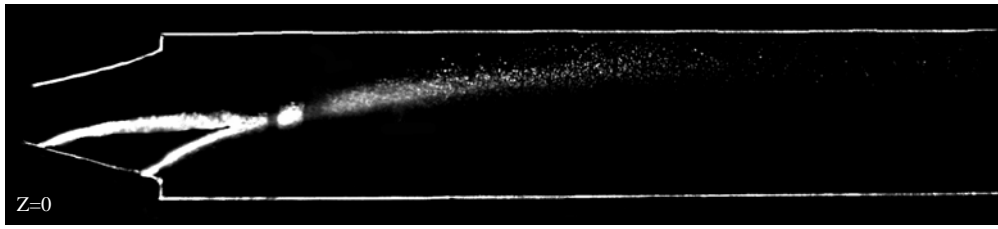


a) Instantaneous side-view NPLS images



b) Instantaneous end-view NPLS images

Fig. 4 Nozzle B ($\theta_j = 40^\circ$, $L_{df} = 4mm$)

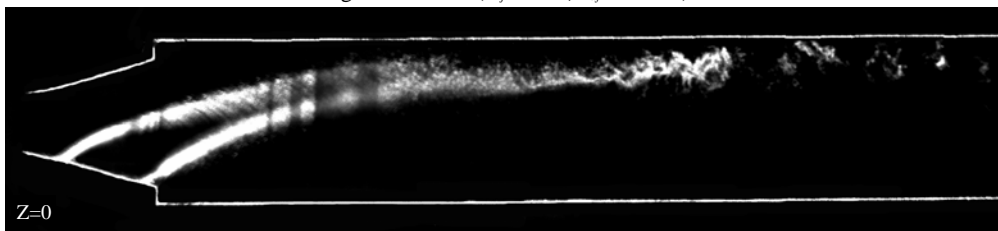


a) Instantaneous side-view NPLS images

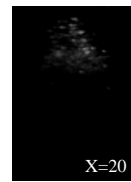
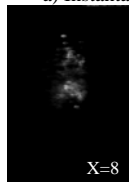


b) Instantaneous end-view NPLS images

Fig. 5 Nozzle C ($\theta_j = 40^\circ$, $L_{inj} = 8mm$)

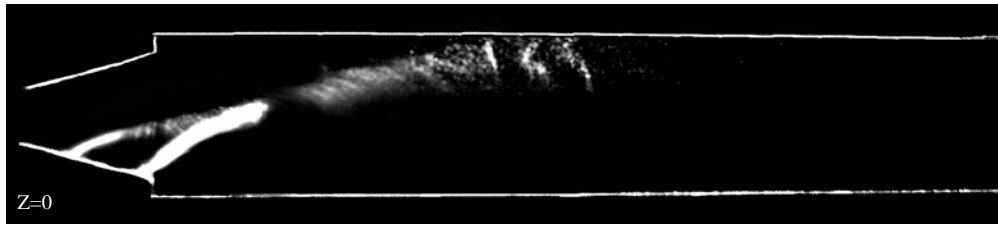


a) Instantaneous side-view NPLS images

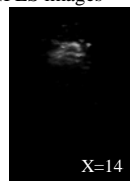


b) Instantaneous end-view NPLS images

Fig. 6 Nozzle D ($\theta_j = 30^\circ$, $L_{inj} = 6mm$)



a) Instantaneous side-view NPLS images



b) Instantaneous end-view NPLS images

Fig. 7 Nozzle E ($\theta_j = 50^\circ$, $L_{inj} = 6mm$)

Comparing Fig. 3a and Fig. 7a, we come to a conclusion that the jet penetration height increases as the injection angle increases. The penetration difference between Nozzle A and Nozzle D is not obvious (Fig. 6a) probably because of the first injector processing error, which results in the poor interaction of the two jets for a distance off the second injector. In other words, the NPLS images can be used as an evaluation method for tiny injector processing.

By visualizing the angled injections flowfield from the end,

the cross-sectional structure of the twin jets is observed. Instantaneous images from streamwise positions X=2, 8, 14 and 20mm are given. Note that the downstream distances of the cross-view images are measured from the nozzle base.

From the Instantaneous spanwise NPLS images of Nozzle A-E, we can see that near the injector exit, two counter-rotating vortex pairs (CVPs) are just forming, then the injected gases are lifted away from the test section floor by the vortex motion. Further downstream the tandem jets attract each other and start

to merge [6], at the same time, the cross section changes from ellipse-shaped to kidney-shaped consequently. This shape is often associated with a vortex structure generated not only by freestream/jet interactions, but also from the interference effects of the twin jet interactions. Due to the increase of the static pressure under the injections, the further from the injections, the weaker the CVPs are, and therefore the cross section becomes less identifiable. From Fig. 3b, we can see that with the structure area increasing with downstream distance, the CRVP is increasing in size with downstream distance. This indicates that diffusive mixing between the injected and primary flows of the nozzle is occurring.

Compared Fig. 3b, Fig. 4b and Fig. 5b, the distance between the CRVP is found to increase with the decreasing of the jet-to-jet spacing. That is to say, vortices become concentrative in a wider jet gap, some of the oncoming fluids slip away from the side of the nozzle. Comparing Fig. 3b, Fig. 6b and Fig. 7b, we notice that Nozzle A creates the largest interfacial surface area to entrain the freestream fluid.

Fig.3(c) shows the top view of NPLS images at various heights from the bottom wall of HYLTE nozzle. From the top view, we can access the lateral spread of the secondary jets. Five pressure measuring orifices placed at the bottom wall are visible at the height $Y=3\text{mm}$. It is a pity that the top quartz glass is too blurred to obtain the flow structures near the front jet, but most of the flowfield is present. The high-pressure recirculation region in front of the second jet appears as curved bands. Behind the backward jet, a pair of symmetric low-pressure "wings" extends downstream along the centerline. The secondary jets are forced to flow away from the wall in the y direction, so the top-view of $Y=8.5$ shows part of the plume region situated under the injectants.

IV. CONCLUSION

The NPLS method which gives a clear identification of mixing structures at side-view, end-view and top-view planes has proved to be a successful flow visualization technique for three-dimensional supersonic flow. In this study, NPLS images are taken at various secondary orifice spaces and injection angles to help qualitatively understand the nature of tandem injectors flowfield. Results show that the secondary fuel injection penetrates deeper while increasing the jet-to-jet spacing, but the counter-rotating vortices are more concentrative which would lead to poor lateral spreading and insufficient mixing of secondary jets. Furthermore, the injectant penetration increases with the increasing of injection angle. The contact cross-sectional area proves to be largest when injecting the secondary gases at the angle of 40 degree. In a word, optimum incident angle and injection gap are essential to enhance the mixing performance of HYLTE nozzle.

REFERENCES

- [1] W. A. Duncan, S. P. Patterson and B. R. Graves, "Overtone research, advanced chemical laser module design," *Proc of SPIE*, Vol. 2119, pp. 46-57, 1994.
- [2] R. J. Driscoll, "Mixing enhancement in chemical lasers, Part I: experiments," *AIAA Journal*, vol. 24, no. 7, pp. 1120-1126, July 1986.
- [3] Yuxin Zhao, Shihe YI and Lifeng Tian, "Supersonic flow imaging via nanoparticles," *Sci China Ser E-Tech Sci*, Vol. 52, no. 12, pp. 3640-3648, 2009.
- [4] Jing Lei, Lin Lai and Zhenguo Wang, "Parameterized design for HYLTE secondary nozzle," *High Power Laser and Particle Beams*, Vol. 19, No. 11, pp. 1766-1770, 2007 (in Chinese).
- [5] Ian A. Waitz, F. E. Marble and E. E. Zukoski, "Investigation of a contoured wall injector for hypervelocity mixing augmentation," *AIAA Journal*, Vol. 31, No. 6, 1993.
- [6] J. U. Schlüter and T. Schönfeld, "LES of jets in cross flow and its application to a gas turbine burner," *Flow, Turbulence and Combustion*, Vol. 65, No. 2, pp. 22-24, 2000.